DRYING MECHANISM OF CAPILLARY-POROUS BODIES

R. Toei and M. Okazaki

UDC 66.047

A new model is proposed for the drying process in capillary-porous solids during the period of falling drying rate. Good agreement is obtained between the theoretical calculations and the experimental results.

INTRODUCTION

During recent years there have been many investigations of the drying rates of various materials. Luikov [3] and co-workers have provided a theoretical basis for a phenomenological hypothesis of combined heat and mass transfer in capillary-porous bodies and have proposed a number of experimental relations for drying processes. Krischer and Mahler [2] have investigated the moisture-transfer coefficient K during the period of constant drying rate without, however, concerning themselves with the period of falling drying rate.

According to the generally accepted theory, during the period of constant drying rate the capillary properties cause the moisture to move toward the surface, where it evaporates. This period continues as long as the surface is wetted by moisture. At the end of this period the drying rate begins to decrease and at this point the surface dries up almost completely. The corresponding mean moisture content of the solid is called the "critical moisture content" and is determined by the dry-air flow conditions and the mass-transfer coefficient. Apparently, before the period of falling drying rate begins, there is almost no internal evaporation of moisture. However, during the latter period vapor transport is as important as moisture transport in the solid. Below, we present the results of an experimental investigation of the drying process in capillary-porous bodies and propose a new simple mathematical model describing the drying mechanism. As the model material we employed an unglazed alumina-based ceramic with sufficiently high thermal conductivity.

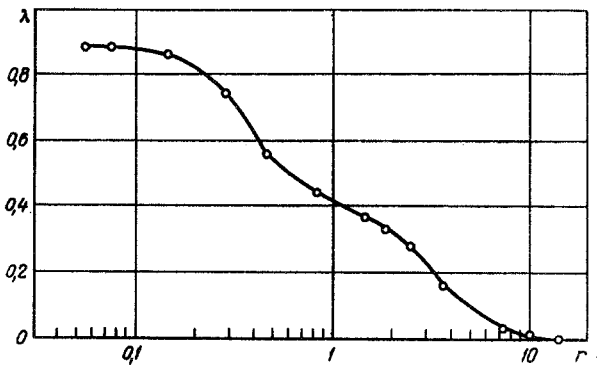

Fig. 1. Pore- (capillary) size distribution curve [r is the pore radius in μ; the ordinates represent the ratio of the cumulative volume of the pores (of the same size) to the total pore volume; ε_T = 0.302; λ_l = 4.0 kcal/h · m · °C; ρ_s = 3.93 g/cm^3; unglazed alumina-based ceramic].

Kyoto University, Japan. Translated from Inzhenerno-Fizicheskii Zhurnal, Vol. 19, No. 3, pp. 464-475, September, 1970. Original article submitted March 5, 1970.

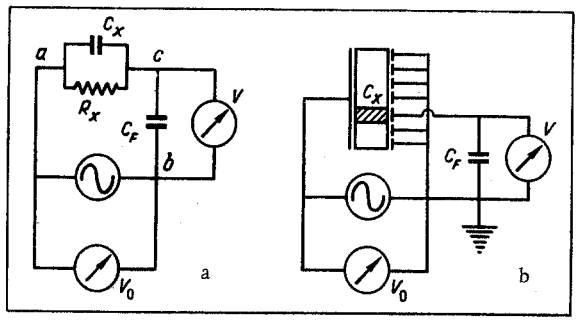

Fig. 2. Equivalent (a) and measuring (b) circuit diagrams.

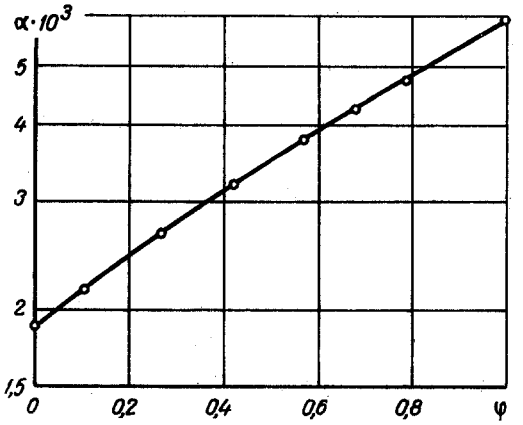

Fig. 3. $\alpha - \varphi$ curve (α and φ are nondimensional).

MATERIALS AND METHOD

Hot air at constant humidity and temperature was blown through a wooden experimental air channel 120 mm wide and 70 mm high. Two premoistened specimens in the form of prisms of unglazed ceramic measuring 30 × 44 mm in cross section and 100 mm in height were placed in sockets in the bottom of the channel and dried from the top. One specimen was used for measuring moisture fields, the other for measuring temperature fields; the measurements were made at frequent intervals. The porosity distribution curve of a specimen investigated with a mercury porosimeter and the physical characteristics of the material are given in Fig. 1.

Determination of Local Moisture Content

For measuring the local moisture content of the specimen we employed the capacitive method proposed in [2] using high-frequency alternating current. This method is based on the fact that the true dielectric constant of a porous material is a function of the moisture content. The electrical conductivity of water increases sharply even at low impurity levels, whereas the dielectric constant is almost unaffected.

The equivalent circuit diagram is shown in Fig. 2a. In this diagram the moist porous specimen is simulated by a parallel circuit consisting of a capacitance C_X and a resistance R_X in conformity with the electrical conductivity of the porous solid. As may be seen from Fig. 2a, the impedances between *a* and c and between *a* and b are given by

$$\dot{Z}_{ac} = \frac{1}{\frac{1}{\dot{Z}_{R_x}} + \frac{1}{\dot{Z}_{C_x}}} = \frac{R_x}{1 - j\omega C_x R_x} \tag{1}$$

and

$$\dot{Z}_{ab} = \dot{Z}_{ac} + \dot{Z}_{bc} = \frac{R_x}{1 - j\omega C_x R_x} - \frac{1}{j\omega C_F}, \tag{2}$$

respectively.

The total current flowing through the specimen will be

$$\dot{I} = \frac{V_0}{\dot{Z}_{ab}}. \tag{3}$$

Then the potential difference between c and b is given by

$$\dot{V} = \dot{I}\dot{Z}_{bc} = \frac{\dot{Z}_{bc}}{\dot{Z}_{ab}} V_0 = \frac{1 - j\omega C_x R_x}{1 - j\omega R_x (C_F + C_x)}, \tag{4}$$

and, consequently,

$$V = \frac{\sqrt{\{\beta^2 + \alpha(\alpha+1)\}^2 + \beta^2}}{\beta^2 + (\alpha+1)^2} V_0, \tag{5}$$

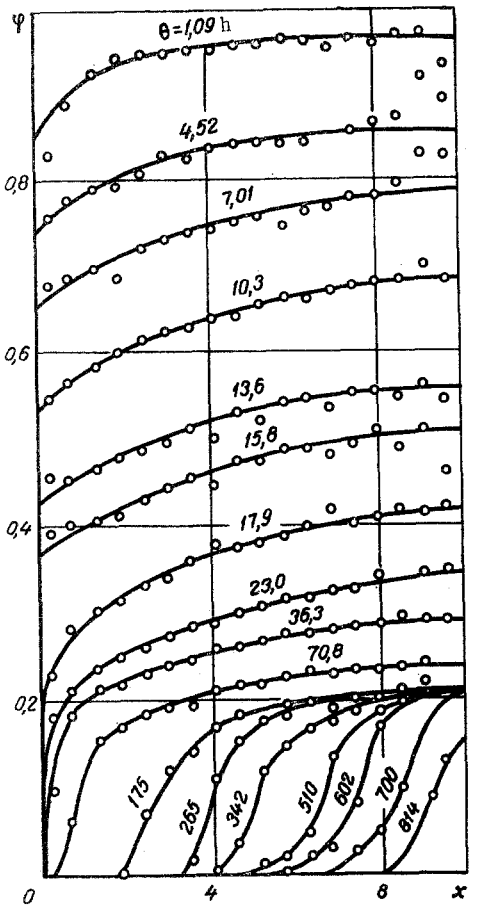

Fig. 4. Moisture content distribution through depth of specimen (moisture field) (x, cm; φ is nondimensional).

where

$$\alpha = \frac{C_x}{C_F}; \tag{6}$$

$$\beta = \frac{1}{\omega C_F R_x}. \tag{7}$$

Knowing V at two frequencies ω_1 and ω_2, we can determine C_X and R_X from Eq. (5). The frequencies ω_1 and ω_2 were 5 and 10 mHz. The measuring circuit is shown in Fig. 2b. Eighteen brass plates 44 mm wide, 5 mm high, and 0.5 mm thick were mounted one above the other on one side of the specimen. On the other side there was a single plate 44 mm wide and 99 mm high. These plates were attached with an epoxy adhesive and served as electrodes. The capacitance C_F was much greater than C_X, so that it could be assumed that the electric lines of force passing through the specimen were parallel. Consequently, the method is accurate enough for determining the local moisture content. A graph of α as a function of φ for one electrode obtained as a result of this experiment is shown in Fig. 3. On the basis of the $\alpha \sim \varphi$ relation for each electrode, it is possible to measure the local moisture content of the specimen continuously. This method is also applicable to layers of granulated and powdered materials.

RESULTS AND DISCUSSION

Period of Constant Drying Rate

On the basis of the moisture distribution curves (Fig. 4) we obtained the characteristic drying rate curves (Fig. 5).

The moisture-transfer coefficient K is determined from the following expression

$$G = -\rho_w \varepsilon_T K \frac{d\varphi}{dx}. \tag{8}$$

Assuming that during the period of constant drying rate moisture is evaporated only from the surface of the specimen, we write the following differential equation

$$\frac{\partial \varphi}{\partial \theta} = \frac{\partial}{\partial x}\left(K \frac{\partial \varphi}{\partial x}\right). \tag{9}$$

Integrating Eq. (9) from x_1 to L, we obtain

$$\int_{x_1}^{L}\left(\frac{\partial \varphi}{\partial x}\right)dx = \frac{\partial}{\partial \theta}\int_{x_1}^{L}\varphi dx = \left[K\frac{\partial \varphi}{\partial x}\right]_{x_1}^{L} = -K\frac{\partial \varphi}{\partial x}\Big|_{x_1}. \tag{10}$$

Hence

$$K = -\frac{\partial}{\partial \theta}\int_{x_1}^{L}\varphi dx \Big/ \frac{\partial \varphi}{\partial x}\Big|_{x_1}. \tag{11}$$

The values of K, calculated from Eq. (11) using the experimental data, are presented in Fig. 6. As may be seen from the figure, the values of K fall by more than 200% as the moisture content decreases from 0.95 to 0.85. Then they remain approximately at the same level for moisture contents from 0.7 to 0.4, falling sharply at lower moisture contents. It is interesting to note that the results obtained by Krischer [1], who used his own model for calculating K, gave a similar picture.

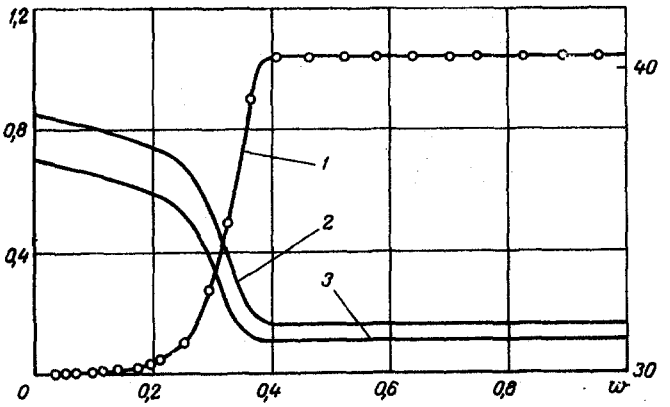

Fig. 5. Characteristic drying curve [w is nondimensional; ordinates: (left) drying rate, kg water/$m^2 \cdot h$; (right) material temperature, °C; velocity of drying agent (air) 10.5 m/sec; temperature 4.16°C; humidity 0.0182 kg water/kg dry air]: 1) drying rate curve; 2) specimen surface temperature curve; 3) temperature curve at bottom of specimen.

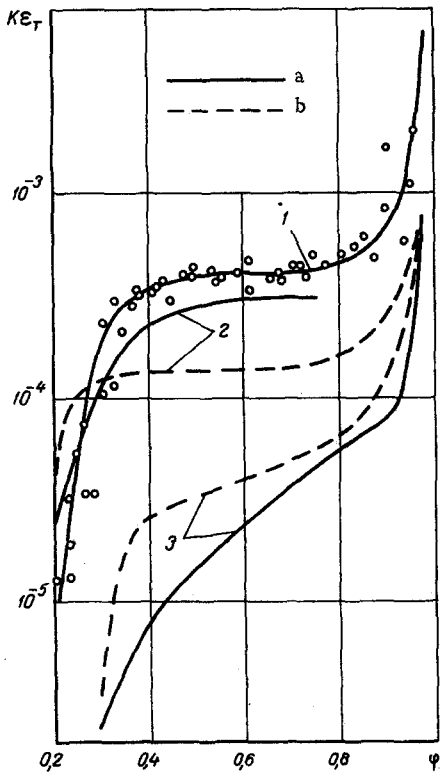

Fig. 6. Moisture-transfer coefficient K as a function of moisture content (experimental data) (φ is nondimensional; $K\varepsilon_T$ is the moisture-transfer coefficient, m^2/h; a and b are values for nonsteady and steady-state drying): 1) Al_2O_3 unglazed ceramic – our data; 2) Eaton's data [2]; 3) Dachsiegel's data.

Critical Moisture Content

It follows from an examination of the moisture fields in Figs. 4 and 5 that the critical moisture content w_c is established at Θ approximately equal to 18 h. At that point the moisture content at the surface is approximately 0.21 and is denoted by φ_c. Clearly, it is reasonable to assume that at $\varphi > \varphi_c$ it is possible to speak of the presence of filtering moisture and that at $\varphi \leq \varphi_c$ all the moisture is in the trapped state. Consequently, the surface moisture content falls to zero as soon as it reaches φ_c, and this point marks the beginning of the period of falling drying rate.

Period of Falling Drying Rate

As noted above, during the period of constant drying rate the moisture transfer is determined by the flow of moisture along the capillaries of the porous body, while during the period of falling drying rate it is determined by the flow of moisture and vapor or, in the last stage, by the flow of vapor alone.

As may be seen from Fig. 4 and 5, the increase in the temperature of the surface and the bottom of the specimen was less than 1°C, while the difference between the surface and bottom temperatures is less than 2°C after Θ = 40 h. Thus, it may be assumed that in this experiment the drying process was isothermal during the period of falling drying rate.

The fact that the temperature of the specimen is constant during the period of constant drying rate, while φ_s is approximately equal to φ_c at w_c, provides a basis for the simplifying assumption that at $\varphi > \varphi_c$ we get moisture transfer and at $\varphi \leq \varphi_c$ vapor transfer or internal evaporation (Fig. 7). Generally speaking, the falling drying rate is chiefly determined by the resistance to vapor transfer in the porous body. A schematic model of the proposed drying mechanism is shown in Fig. 7. The solid is divided into three zones: a dry zone, an internal evaporation zone, and a moisture transfer zone.

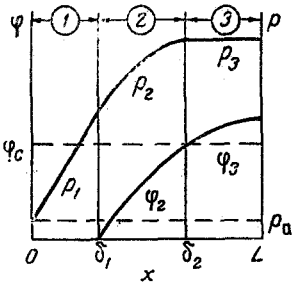

Fig. 7. Three-zone model (x, cm; φ is nondimensional; p atm abs): 1) dry zone; 2) internal evaporation zone; 3) moisture transfer zone.

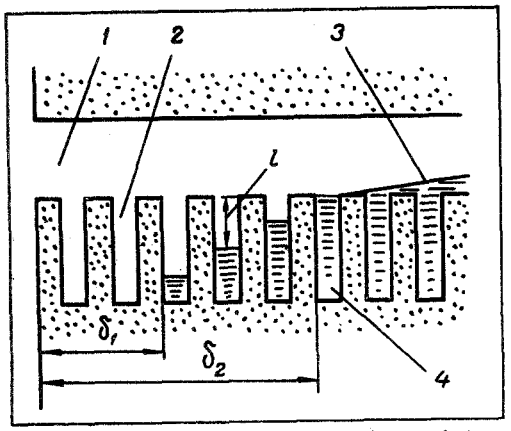

Fig. 8. Schematic model of the moisture distribution in the capillaries (period of falling drying rate): 1) primary capillaries; 2) secondary capillaries; 3) filtering moisture; 4) trapped moisture.

Dry Zone ($0 \leq x < \delta_1$). In this zone we get only vapor transfer described by the following equation

$$\varepsilon_T \frac{\partial p_1}{\partial \theta} = \frac{D_v'}{\mu_l} \cdot \frac{\partial^2 p_1}{\partial x^2}, \tag{12}$$

where

$$D_v' = \frac{D_v \pi}{(\pi - p)_{lm}} = \frac{D_v \pi}{(p_{air})_{lm}}. \tag{13}$$

The expression on the left of Eq. (12) is usually much less than the expression on the right; accordingly, it may be assumed approximately equal to zero.

Internal Evaporation Zone ($\delta_1 \leq x < \delta_2$). Assuming that vapor transfer is determined by the partial vapor-pressure gradient, we can write the following equation

$$\frac{\varepsilon M}{RT_{av}} \cdot \frac{\partial p_2}{\partial \theta} = \frac{D_v' M}{\mu_l R T_{av}} \frac{\partial^2 p_2}{\partial x^2} + [\text{internal evaporation rate}] \tag{14}$$

The internal evaporation rate is calculated as follows. A schematic model of a capillary-porous solid is shown in Fig. 8. Filtering moisture fills the primary capillaries and trapped moisture the secondary capillaries. Whereas the funicular moisture can flow through the primary capillaries, the pendular moisture cannot and can be removed only by evaporation (internal) and vapor transfer along the capillaries. We now assume that the moisture content at which all the secondary capillaries are filled with moisture, corresponds to φ_c. At points where the moisture content is less than φ_c we get only evaporation of moisture and vapor transfer, moisture transfer being almost nonexistent. On the other hand, at points where the moisture content is greater than φ_c moisture transfer predominates.

We assume that the distance l (see Fig. 8) is proportional to $(\varphi_c - \varphi_2)$ and that the resistance to internal evaporation in a secondary capillary is proportional to l. The internal evaporation rate is then written as follows

$$[\text{internal evaporation rate}] = \frac{k'}{\varphi_c - \varphi_2}(p_s - p_2). \tag{15}$$

Substituting expression (15) in Eq. (14), we obtain

$$\frac{\varepsilon M}{RT_{av}} \cdot \frac{\partial p_2}{\partial \theta} = \frac{D_v' M}{\mu_l R T_{av}} \cdot \frac{\partial^2 p_2}{\partial x^2} + \frac{k'}{\varphi_c - \varphi_2}(p_s - p_2), \tag{16}$$

$$-\varepsilon_T \rho_w \frac{\partial \varphi_2}{\partial \theta} = \frac{k'}{\varphi_c - \varphi_2}(p_s - p_2). \tag{17}$$

In this case the expression on the left of Eq. (16) is much less than the expression on the right and consequently can be neglected.

Moisture Transfer Zone ($\delta_2 \leq x \leq L$). In the initial stage of the period of falling drying rate we have moisture transfer in the specimen, where $\varphi_3 \geq \varphi_c$, and for this zone we can write the following equation

$$\frac{\partial \varphi_3}{\partial \theta} = \frac{\partial}{\partial x}\left(K \frac{\partial \varphi_3}{\partial x}\right). \tag{18}$$

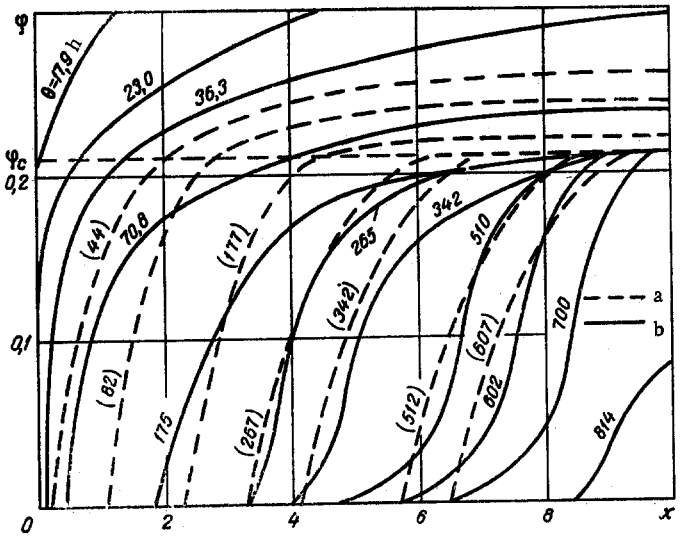

Fig. 9. Comparison of theoretical (a) and experimental (b) moisture field curves (x, cm; φ is nondimensional.

The initial and boundary conditions for Eqs. (12)-(18) are as follows.

Initial conditions:

$$\text{at } \theta = 0 \qquad \varphi_3 = \varphi_{crit}(x), \tag{19}$$

$$\delta_1 = \delta_2 = 0. \tag{20}$$

$\varphi_{crit}(x)$ can be determined from Eq. (8) and Fig. 6, if φ_s is taken equal to φ_c.

Boundary conditions:

$$\text{at } x = 0 \qquad \frac{D_v' M}{\mu_l R T_{av}} \frac{\partial p_1}{\partial x} = k_g (p_1 - p_a), \tag{21}$$

$$\varphi_1 = 0; \tag{22}$$

$$\text{at } x = \delta_1 \qquad p_1 = p_2, \tag{23}$$

$$\frac{\partial p_1}{\partial x} = \frac{\partial p_2}{\partial x}, \tag{24}$$

$$\varphi_2 = 0. \tag{25}$$

$$\text{at } x = \delta_2 \qquad \frac{D_v' M}{\mu_l R T_{av}} \cdot \frac{\partial p_2}{\partial x} = \varepsilon_T K \rho_w \frac{\partial \varphi_3}{\partial x}, \tag{26}$$

$$\varphi_2 = \varphi_3 = \varphi_c, \tag{27}$$

$$p_2 = p_s = \text{const}; \tag{28}$$

$$\text{at } x = L \qquad \frac{\partial \varphi_3}{\partial x} = 0. \tag{29}$$

Solutions of Partial Differential Equations

The system of partial differential equations obtained above is solved numerically with the following assumptions:

1) the left sides of Eqs. (12) and (16) are negligibly small;

2) the moisture-transfer coefficient K is assumed constant;

3) the expression for the internal evaporation rate can be approximately linearized by introducing the constants k" and c' and can be written in the following form

$$\frac{k'}{\varphi_c - \varphi_2}(p_s - p_2) \cong k''(\varphi_2 + c')(p_s - p_2); \tag{30}$$

4) the boundary conditions of the third kind of Eq. (21) are approximated by conditions of the first kind.

Then the following changes of variables are made in Eqs. (12)-(18)

$$P=\frac{p-p_a}{p_s-p_a},\quad \Phi=\frac{\varphi}{\varphi_c},\quad \xi_1=\frac{x}{\delta_1},\quad \xi_2=\frac{x-\delta_2}{L-\delta_2},$$
$$\Delta=\frac{\delta}{L},\quad C=\frac{c'}{\varphi_c},\quad \Theta=F\theta. \tag{31}$$

We introduce the notation

$$A=\frac{D_v'M}{\mu_l RT_{av}L^2k''\varphi_c},\qquad D=\frac{K\rho_w\varepsilon_T}{L^2k''(p_s-p_a)},$$
$$E=\frac{\mu_l RT_{av}\rho_w\varepsilon_T K\varphi_c}{D_v'M(p_s-p_a)},\qquad F=\frac{k''(p_s-p_a)}{\varepsilon_T\rho_w}. \tag{32}$$

As a result we obtain the following system of equations

$$0\leq\xi_1<1,\quad \frac{\partial^2P_2}{\partial\xi_1^2}=0; \tag{33}$$

$$0\leq\xi_2<1,\quad \frac{A}{(\Delta_2-\Delta_1)^2}\cdot\frac{\partial^2P_2}{\partial\xi_2^2}+(1-P_2)(\Phi_2+C)=0, \tag{34}$$

$$-\frac{\partial\Phi_2}{\partial\Theta}+\frac{1}{\Delta_2-\Delta_1}\left\{(1-\xi_2)\frac{d\Delta_1}{d\Theta}+\xi_2\frac{d\Delta_2}{d\Theta}\right\}\frac{\partial\Phi_2}{\partial\xi_2}=(1-P_2)(\Phi_2+C); \tag{35}$$

$$0\leq\xi_3\leq1,\quad \frac{\partial\Phi_3}{\partial\Theta}+\frac{\xi_3-1}{1-\Delta_2}\cdot\frac{d\Delta_2}{d\Theta}\cdot\frac{\partial\Phi_3}{\partial\xi_3}=\frac{D}{(1-\Delta_2)^2}\cdot\frac{\partial^2\Phi_2}{\partial\xi_3^2}. \tag{36}$$

For simplicity, in these equations ε is assumed approximately equal to ε_T. We write the initial and boundary conditions for this system:

at $\Theta=0$

$$\Phi_3=\Phi_{crit}(\xi_3), \tag{37}$$
$$\Delta_1=\Delta_2=0; \tag{38}$$

at $\xi_1=1,\quad \xi_2=0$

$$P_1=P_2, \tag{39}$$
$$\Phi_2=0, \tag{40}$$
$$\frac{1}{\Delta_1}\cdot\frac{\partial P_1}{\partial\xi_1}=\frac{1}{\Delta_2-\Delta_1}\cdot\frac{\partial P_2}{\partial\xi_2}; \tag{41}$$

at $\xi_2=1,\quad \xi_3=0$

$$P_2=1, \tag{42}$$
$$\frac{1}{\Delta_2-\Delta_1}\cdot\frac{\partial P_2}{\partial\xi_2}=\frac{E}{1-\Delta_2}\cdot\frac{\partial\Phi_3}{\partial\xi_3}, \tag{43}$$
$$\frac{\partial\Phi_2}{\partial\xi_2}=0, \tag{44}$$
$$\Phi_2=\Phi_3=1; \tag{45}$$

at $\xi_3=1$

$$\frac{\partial\Phi_3}{\partial\xi_3}=0, \tag{46}$$
$$P_3=1. \tag{47}$$

Equation (44) is the supplementary condition of smooth displacement of δ_2.

This system of equations can be solved numerically by the method of moments proposed by Yamada [4], the essence of which consists in the following. We write the solution for P and Φ (respectively) in the form of polynomials ξ with unknown coefficients that are functions of Θ and substitute these polynomials in the system of partial differential equations. The number of different integral moments for ξ is the same as the number of unknown coefficients and, accordingly, we obtain a new system of first-order ordinary

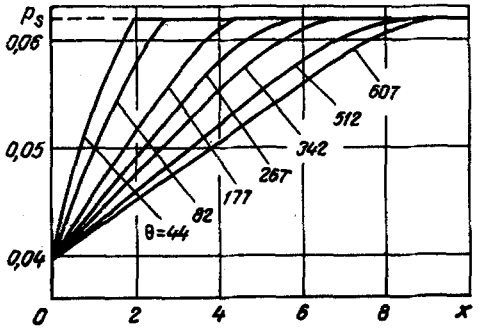

Fig. 10

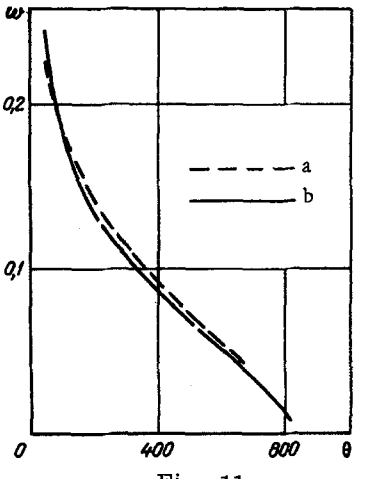

Fig. 11

Fig. 10. Theoretical vapor-pressure curves (x, cm; p is the water-vapor pressure in the primary capillaries, atm abs).

Fig. 11. Comparison of theoretical (a) and experimental (b) values of the mean moisture content (Θ, h; w is nondimensional; w_c = 0.366, nondimensional; Θ = 17.9 h).

differential equations in the same unknown coefficients. Hence the problem reduces to solving the latter system of differential equations by some numerical method.

As the approximate solutions for P and Φ we selected second-order polynomials ξ. The calculated values of the moisture content φ and the partial pressure of water vapor in the specimen are presented in Figs. 9 and 10, respectively. In the solution we employed the following numerical values:

$$c' = 0.0473 \text{ (nondimen.)}; \quad k'' = 0{,}935 \text{ g/cm}^3 \cdot \text{atm abs} \cdot \text{h};$$

$$T_{av} = 310\,^{\circ}\text{K}; \quad K = 0{,}233 \text{ cm}^2/\text{h};$$

$$\mu_l = 4{,}5 \text{ (nondimen.)}; \quad \varepsilon_T = 0{,}30 \text{ (nondimen.)}.$$

Values of k', and then k" and c', were calculated from Fig. 4 and Eqs. (16), (17) as

$$k' = \frac{D_v'}{\mu_l R T_{av}} \cdot \frac{\partial^2}{\partial x^2} \left\{ (\varphi_c - \varphi_2) \frac{\partial \varphi_2}{\partial \theta} \right\} \Big/ \left(\frac{\partial \varphi_2}{\partial \theta} \right). \tag{48}$$

In Fig. 11 the analytic and experimental relations between the mean moisture content and drying time are compared for the period of falling drying rate. In Fig. 9 it is possible to detect certain discrepancies between the calculated and experimental values. This can be attributed to the fact that we employed constants K and k', and then k" and c', that represent values corresponding to the middle of the period of falling drying rate. At lesser values of the moisture content it is also possible to detect moisture adsorption effects.

Despite the rather rough assumptions mentioned above, the calculated values are in good agreement with the experimental data. In this connection, the model and mathematical apparatus proposed for investigating the drying mechanism and hence the moisture and vapor transport mechanism in a capillary-porous solid may be regarded as acceptable.

NOTATION

c' is the constant in Eq. (30), nondimensional;
C_X is the specimen capacitance, pF;
C_F is a standard capacitance, pF;
D_V is the coefficient of diffusion of water vapor into air, cm²/h;
I is current, A;
k' is the internal evaporation coefficient, g/cm³ · atm · h;
k" is the constant in Eq. (30), g/cm³ · atm · h;

k_g is the mass-transfer coefficient, g/cm^3 · atm · h;
l is the length of the diffusion zone in a secondary capillary, cm;
L is the specimen depth, cm;
M is the molecular weight of water, g/mole;
p is the water-vapor pressure, atm abs;
p_a is the water-vapor pressure in the drying agent, atm abs;
p_s is the saturated vapor pressure, atm abs;
R is the gas constant, cm^3 · atm/mole · °K;
R_x is electrical resistance, ohm;
r is the capillary radius, μ;
t is temperature, °C;
T is absolute temperature, °K;
V is voltage, V;
w is the mean mixture content, cm^3 water/cm^3 capillary volume;
w_c is the critical moisture content, cm^3 water/cm^3 capillary volume;
x is the distance from the surface (of the specimen), cm;
Z is impedance, ohm;
δ is the distance from the surface to the moving interface, cm;
ε is porosity, nondimensional;
ε_T is the total porosity, nondimensional;
Θ is time, h;
K is the moisture-transfer coefficient, m^2/h, cm^2/h;
μ_l is the path factor for vapor diffusion through capillaries [1] ($\mu_l = \mu_{l\,diff}/\varepsilon_T$), nondimensional;
π is the total pressure, atm abs;
λ_l is the thermal conductivity of the solid, kcal/h · m · °C;
ρ_s is the true density, g/cm^3;
ρ_w is the density of water, g/cm^3;
φ is the local moisture content, the relative volume ratio of moisture to total capillary volume, cm^3 water/cm^3 capillary volume;
φ_c is the local moisture content at w_c, cm^3 water/cm^3 capillary volume;
φ_{crit} is the local critical moisture content, cm^3 water/cm^3 capillary volume;
φ_s is the local moisture content at the surface, cm^3 water/cm^3 capillary volume;
ω is frequency, 1/sec.

LITERATURE CITED

1. O. Krischer, Die wissenschaftlichen Grundlagen der Trocknungstechnik, 2nd ed., Springer–Verlag, Berlin (1963).
2. O. Krischer and K. Mahler, V.D.I.-Forsch., Heft 473 (1959).
3. A. V. Luikov, Heat and Mass Transfer in Capillary-Porous Bodies, Pergamon, Oxford (1966).
4. H. Yamada, Reports of Res. Inst. Fluid Eng., Kyushu Univ., Japan, 6, No. 2, 42 (1950).